Available online at www.sciencedirect.com
ScienceDirect
Ocean Modelling 20 (2008) 223–239
Ocean Modelling
www.elsevier.com/locate/ocemod

Towards a mesoscale eddy closure

Carsten Eden [a,*], Richard J. Greatbatch [a,b]

[a] IFM-GEOMAR, Dusternbrooker Weg 20, 24105 Kiel, Germany
[b] Dalhousie University, Halifax, Canada

Received 12 June 2007; received in revised form 10 September 2007; accepted 10 September 2007
Available online 25 September 2007

Abstract

A turbulence closure for the effect of mesoscale eddies in non-eddy-resolving ocean models is proposed. The closure consists of a prognostic equation for the eddy kinetic energy (EKE) that is integrated as an additional model equation, and a diagnostic relation for an eddy length scale (L), which is given by the minimum of Rhines scale and Rossby radius. Combining EKE and L using a standard mixing length assumption gives a diffusivity (K), corresponding to the thickness diffusivity in the [Gent, P.R., McWilliams, J.C. 1990. Isopycnal mixing in ocean circulation models. J. Phys. Oceanogr. 20, 150–155] parameterisation. Assuming downgradient mixing of potential vorticity with identical diffusivity shows how K is related to horizontal and vertical mixing processes in the horizontal momentum equation, and also enables us to parameterise the source of EKE related to eddy momentum fluxes.

The mesoscale eddy closure is evaluated using synthetic data from two different eddy-resolving models covering the North Atlantic Ocean and the Southern Ocean, respectively. The diagnosis shows that the mixing length assumption together with the definition of eddy length scales is valid within certain limitations. Furthermore, implementation of the closure in non-eddy-resolving models of the North Atlantic and the Southern Ocean shows consistently that the closure has skill at reproducing the results of the eddy-resolving model versions in terms of EKE and K.

1. Introduction

In many state-of-the-art, non-eddy-resolving ocean models the so-called thickness diffusivity K appropriate to the Gent and McWilliams (1990) (GM) parameterisation is used. This lateral diffusivity is meant to account for the advective effect of the turbulent lateral mixing by mesoscale eddies. In the GM parameterisation, the value of K has to be specified and is typically chosen in non-eddy-resolving ocean models as o(1000 m^2/s). It is clear that K should have horizontal (Visbeck et al., 1997) and vertical structure (Ferreira et al., 2005) (see also the theory of Killworth, 1997 based on linear instability theory) and recently, Eden (2007) and Eden (2006) have diagnosed K in eddy-resolving models of the North Atlantic and the Southern Ocean and indeed find significant horizontal and vertical variations, with magnitudes ranging from zero to 5000 m^2/s. Furthermore,

* Corresponding author. Tel.: +49 431 600 4177; fax: +49 431 600 4012.
E-mail address: ceden@ifm-geomar.de (C. Eden).

1463-5003/$ - see front matter
doi:10.1016/j.ocemod.2007.09.002

modern ocean models are beginning to incorporate spatially varying thickness diffusivities, but in a rather ad hoc manner (Gnanadesikan et al., 2006; Danabasoglu and Marshall, 2007).

It is the aim of the present study to derive a physically consistent parameterisation for the effect of mesoscale eddies in the interior ocean that goes beyond a constant prescribed value of K. It is based on a mixing length approach, first proposed for geophysical application by Green (1970) and Stone (1972), and takes account of the turbulent energy budget. A first step towards such a closure was presented by Canuto and Dubovikov (2006), together with a series of follow-on papers. Note, however, that these papers are the subject of a controversy (McDougall et al., 2007; Canuto and Dubovikov, 2007). In contrast to Canuto and Dubovikov (2006), we discuss here the simplest possible of such parameterisations only, further refinements being postponed to later studies. The simple closure is tested in numerical ocean models. In addition to the closure for the diffusivity (corresponding to thickness diffusivity), the implications of the closure for the treatment of the horizontal momentum equations in coarse resolution models are also discussed.

We begin in Section 2 by discussing the GM parameterisation and the need to specify the thickness diffusivity, while in Section 3 we present a simple closure based on a mixing length approach going back to Prandtl (1925); namely, a parameterised but prognostic eddy kinetic energy budget and a diagnostic relation for an eddy length scale. In Section 4, we evaluate the performance of the closure using two realistic eddy-resolving ocean models and their non-eddy-resolving counterparts, and in the last section we summarize and discuss our conclusions. We explore the consequences of our closure for the momentum budget in an appendix.

2. Buoyancy mixing in the ocean

We start with the Boussinesq approximation, neglect any complication from a non-linear equation of state and use b as buoyancy with $b = -g(\rho - \rho_0)/\rho_0$ where ρ_0 denotes a constant reference density. The averaged buoyancy budget is then given by

$$\frac{\partial}{\partial t}\bar{b} + \bar{\boldsymbol{u}} \cdot \nabla \bar{b} + \nabla \cdot \overline{\boldsymbol{u}'b'} = \overline{Q} \tag{1}$$

where the buoyancy is decomposed into mean (overbars) and fluctuating parts (primes) $b = \bar{b} + b'$ before averaging, and equivalently for velocity $\boldsymbol{u} = \bar{\boldsymbol{u}} + \boldsymbol{u}'$. The instantaneous diabatic forcing is given by Q and $\overline{\boldsymbol{u}'b'}$ denotes the eddy buoyancy flux. Following the Transformed Eulerian Mean (TEM) framework by Andrews and McIntyre (1976) we decompose $\overline{\boldsymbol{u}'b'}$ as

$$\overline{\boldsymbol{u}'b'} = -K_{\mathrm{dia}} \nabla \bar{b} + \boldsymbol{B} \times \nabla \bar{b} + \nabla \times \boldsymbol{\theta} \tag{2}$$

with a diapycnal diffusivity $K_{\mathrm{dia}} = -|\nabla \bar{b}|^2 (\overline{\boldsymbol{u}'b'} - \nabla \times \boldsymbol{\theta}) \cdot \nabla \bar{b}$ and a rotational flux given by the vector potential $\boldsymbol{\theta}$, which drops out in the divergence of $\overline{\boldsymbol{u}'b'}$ in the mean tracer budget. Eden et al. (2007a) showed that $\boldsymbol{\theta}$ can be chosen such that $K_{\mathrm{dia}} = 0$ for steady and adiabatic flow ($Q = 0$). Since Q is indeed small in the interior of the ocean, we assume for now that we can put $K_{\mathrm{dia}} = 0$. We will also assume that a rotational flux according to Eden et al. (2007a) has been removed from $\overline{\boldsymbol{u}'b'}$, and do not explicitly indicate the rotational part of the flux in what follows.

The second part of the flux decomposition in Eq. (2) introduces a vector streamfunction $\boldsymbol{B}$ for the eddy-induced velocity $\boldsymbol{u}^*$. Since $\nabla \cdot \overline{\boldsymbol{u}'b'} = \nabla \times \boldsymbol{B} \cdot \nabla \bar{b}$, the curl of $\boldsymbol{B}$ acts like an eddy-induced, three-dimensional advection velocity which adds to the Eulerian mean velocity $\bar{\boldsymbol{u}}$ in Eq. (1) (see also McDougall and McIntosh, 2001 for a discussion of $\boldsymbol{u}^*$). The vector streamfunction $\boldsymbol{B}$ can be written (using the gauge condition $\boldsymbol{B} \cdot \nabla \bar{b} = 0$)

$$\boldsymbol{B} = -|\nabla \bar{b}|^{-2} \overline{\boldsymbol{u}'b'} \times \nabla \bar{b} = |\nabla \bar{b}|^{-2} \begin{pmatrix} \overline{v'b'}\bar{b}_z - \overline{w'b'}\bar{b}_y \\ \overline{w'b'}\bar{b}_x - \overline{u'b'}\bar{b}_z \\ \overline{u'b'}\bar{b}_y - \overline{v'b'}\bar{b}_x \end{pmatrix} \approx \bar{b}_z^{-1} \begin{pmatrix} \overline{v'b'} \\ -\overline{u'b'} \\ \overline{u'b'}\frac{\bar{b}_y}{\bar{b}_z} - \overline{v'b'}\frac{\bar{b}_x}{\bar{b}_z} \end{pmatrix} \tag{3}$$

Note that the last approximation in Eq. (3) is valid only for $|\bar{b}_z| \gg |\nabla_{\mathrm{h}} \bar{b}|$, a good approximation in the ocean interior. To use the streamfunction $\boldsymbol{B}$ given by Eq. (3) in a coarse resolution model, the horizontal eddy buoyancy fluxes, $\overline{\boldsymbol{u}_h' b'}$, have to be parameterized. The GM parameterization corresponds to assuming that $\overline{\boldsymbol{u}_h' b'}$ is directed down the horizontal gradient of the mean buoyancy

$$\overline{\boldsymbol{u}_h' b'} \stackrel{!}{=} -K\bar{\nabla}_h b \tag{4}$$

Gent and McWilliams (1990) introduced the diffusivity K as a prescribed constant of o(1000 m^2/s) and Gent et al. (1995) showed that for $K > 0$ the parameterization releases available potential energy from the mean state. However, it was demonstrated for instance in Eden et al. (2007b) and Eden (2006) (by evaluating $K = -|\nabla_h \bar{b}|^{-2}\overline{\boldsymbol{u}_h' b'} \cdot \nabla_h \bar{b}$ from numerical models) that K shows strong horizontal and vertical variations, and, in addition, that K should really be a tensor. Note that the latter complication is ignored here, we will first concentrate on a simple closure for a scalar diffusivity K, as a first step beyond a constant value of K and leave a possible extension to anisotropic mixing for a future application. We will also show how lateral and vertical mixing in the momentum equation can be related to K in Appendix A.

3. A simple mesoscale eddy closure

A simple closure for the horizontal eddy buoyancy fluxes in the ocean is given by adopting the downgradient parameterisation Eq. (4) and assuming

$$K \stackrel{!}{=} LU \tag{5}$$

where L denotes a characteristic eddy length scale and U a characteristic eddy velocity which is related to the eddy kinetic energy $\bar{e}$ (EKE) by $U = \bar{e}^{1/2}$. This simple closure goes back to Prandtl (1925), has first been proposed for geophysical application in the pioneering work by Green (1970) and Stone (1972), and also forms the basis of many planetary boundary layer turbulence closures (e.g. Rodi, 1980; Mellor and Yamada, 1982; Gaspar et al., 1990). In such closures, U is given by a prognostic EKE budget, while the length scale is either taken from diagnostic relations or from prognostic budgets as well.

The relevant EKE budget for the large-scale oceanic flow is given by

$$\frac{\partial}{\partial t}\bar{e} + \bar{\boldsymbol{u}} \cdot \nabla\bar{e} = \overline{S} + \overline{b'w'} - \epsilon - \nabla \cdot \boldsymbol{M} \tag{6}$$

On the right hand side of the equation, one finds the energy production term $\overline{S} = -\overline{\boldsymbol{u}'u'} \cdot \nabla_h \bar{u} - \overline{\boldsymbol{u}'v'} \cdot \nabla_h \bar{v}$ related to the eddy momentum fluxes and describing the exchange with mean kinetic energy, the energy production term $\overline{b'w'}$ related to baroclinic instability and the dissipation of EKE denoted by ϵ. In addition, there is the divergence of a flux $\boldsymbol{M}$ containing advection of EKE by the fluctuating flow and correlations between pressure and velocity fluctuations, $\nabla \cdot \boldsymbol{M} = \nabla \cdot \overline{\boldsymbol{u}'e} + \nabla \cdot \overline{\boldsymbol{u}'p'}$.

In the next couple of sections we discuss simple parameterisations for the terms on the right hand side of Eq. (6) and diagnostic relations for the eddy length scale L. The parameterized EKE budget can then be integrated in a coarse resolution model to obtain the characteristic eddy velocity scale. Using the length scale L, the diffusivity K can be calculated. An assumption of downgradient mixing of potential vorticity further allows us to relate K to the horizontal and vertical mixing in the mean momentum budget, an issue discussed in Appendix A. Note that we discuss here the simplest possible parameterisations only, further refinements are postponed.

3.1. Energy production related to baroclinic instability

We have assumed in Section 2 that $K_{dia} = 0$. From that assumption and using the downgradient parameterisation for $\overline{\boldsymbol{u}_h' b'}$, Eq. (4), we find for the baroclinic instability energy production term

$$\overline{b'w'} = K\frac{|\nabla_h \bar{b}|^2}{N^2} \tag{7}$$

with $N^2 = \bar{b}_z$. This term has a singularity for $N = 0$ as a consequence of the assumption $K_{\rm dia} = 0$ and Eq. (7) should be applied in the stratified interior of the ocean only. Approaching the near surface mixed layer, it is clear that the eddy-induced diapycnal diffusivity $K_{\rm dia}$ will become non-zero and we find

$$\overline{b'w'} = (K - K_{\rm dia})\frac{|\nabla_{\rm h}\bar{b}|^2}{N^2} - K_{\rm dia}N^2 \tag{8}$$

It becomes clear that for $N^2 \to 0$ the diapycnal diffusivity and K should become equal to prevent a singularity. Thus, for simplicity, we set

$$K_{\rm dia} = K_{\rm dia}(N^2) \quad \text{with } K_{\rm dia} = \begin{cases} 0 & \text{for finite } N^2 \\ K & \text{for } N^2 \to 0 \end{cases} \tag{9}$$

Issues concerning the parameterisation of $K_{\rm dia}$ in the mixed layer are discussed briefly in the discussion section.

3.2. Dissipation

The dissipation in homogeneous three-dimensional turbulence is often parameterized as

$$\epsilon = \bar{e}^{3/2}L^{-1} \tag{10}$$

This closure is based on dimensional arguments and on the assumption of a turbulent energy cascade. The cascade is thought to extend over a certain (inertial) range in the wavenumber spectrum in which turbulent energy is fluxed from large scales (L) at which is is generated, to small scales at which it is dissipated by molecular viscosity. This flux of energy stays the same at all scales (smaller than L) and equals the dissipation ϵ in steady state. Since the flux at larger scales of the cascade should not depend on details of dissipation at small scales, the flux (or ϵ) depends on the energy and length scale of the flow at the large scales only (the large scales dominate the total energy, $\bar{e}$). Eq. (10) is simply the only combination of e and L which yields dimensions identical to ϵ. There is large experimental support for the validity of Eq. (10) in three-dimensional turbulence.

For quasi-geostrophic flow in the ocean, however, there is recent evidence from satellite altimeter data (Scott and Wang, 2005) and eddy-resolving modelling (Schlösser and Eden, 2007), that the kinetic energy cascade is upscale, i.e. turbulent kinetic energy is fluxed from small scales to large scales, in accordance to the inverse energy cascade in classical two-dimensional turbulence theory (e.g. Salmon, 1998). However, still the same arguments which have led to Eq. (10) for three-dimensional turbulence are possible for the two-dimensional case, i.e. for an inverse energy cascade as suggested by e.g. Larichev and Held (1995), Held and Larichev (1996) and Salmon (1998). We therefore use Eq. (10) as a parameterisation for the dissipation of EKE in the present application.

3.3. Radiation

A meaningful physical interpretation of $\overline{\boldsymbol{u}'e}$ and $\overline{\boldsymbol{u}'p'}$ both for the planetary boundary layer case and for the present application is given by wave radiation, i.e. inertio-gravity waves in the boundary layer case and Rossby waves for QG dynamics. This process is often simply parameterised as isotropic diffusion of EKE

$$\nabla \cdot \overline{\boldsymbol{u}'e} + \nabla \cdot \overline{\boldsymbol{u}'p'} = \nabla \cdot \boldsymbol{M} = -\nabla_{\rm h} \cdot K\nabla_{\rm h}\bar{e} \tag{11}$$

Note that one might also include vertical diffusion of EKE, but certainly with smaller vertical diffusivity as given by K. Although it is for numerical integration certainly useful to have lateral and vertical diffusion, such an isotropic diffusion might only be a very rough first order parameterisation for the Rossby wave radiation of eddy energy. Note that by using a diffusive parameterisation, energy that is generated at small scales, as is usually the case, will be dispersed to larger scales by the diffusion operator, analogous to an inverse energy cascade.

3.4. Energy production related to eddy momentum fluxes

For the energy production term $\overline{S}$ we need to parameterize the eddy momentum fluxes, $\overline{\boldsymbol{u}'\boldsymbol{u}'_{\rm h}}$. It is clear that $\overline{\boldsymbol{u}'\boldsymbol{u}'_{\rm h}}$ is not simply mixed down the gradient of mean momentum $\bar{\boldsymbol{u}}_{\rm h}$. Instead, it is often argued that potential vorticity is mixed and not the momentum itself (Green, 1970; Marshall, 1981) and we follow this suggestion here. A short outline of our approach is the following. By comparing the potential vorticity budget derived from the mean momentum and mean buoyancy equations with the mean of the instantaneous potential vorticiy budget, we are able to relate the divergences of the eddy momentum fluxes to the parameterised horizontal fluxes of buoyancy and potential vorticity. This parameterisation for the divergences of the eddy momentum fluxes will then be used to derive an expression for $\overline{S}$ (the exchange with EKE) in the mean kinetic energy (MKE) budget, which can then finally be used in our eddy closure. This result is obtained by assuming that potential vorticity is mixed down the mean potential vorticity gradient having the same diffusivity as for buoyancy given by Eq. (5).

We begin by noting that the budget of MKE is obtained by scalar multiplication of $\bar{\boldsymbol{u}}_\mathrm{h}$ with the mean momentum budget to yield

$$\frac{\partial}{\partial t}\overline{E} + \bar{\boldsymbol{u}}\cdot\nabla\overline{E} = -\nabla\cdot\bar{\boldsymbol{u}}\bar{p} - \bar{\boldsymbol{u}}_\mathrm{h}\cdot\boldsymbol{F}_u + \bar{b}\bar{w} + \epsilon_E \tag{12}$$

where $\overline{E} = \frac{1}{2}|\bar{\boldsymbol{u}}_\mathrm{h}|^2$ denotes MKE, ϵ_E frictional terms and where $\boldsymbol{F}_u = (\nabla_\mathrm{h}\cdot\overline{u'\boldsymbol{u}'_\mathrm{h}}, \nabla_\mathrm{h}\cdot\overline{v'\boldsymbol{u}'_\mathrm{h}})^\mathrm{T}$ denotes the vector composed of the divergence of the zonal and meridional eddy momentum fluxes (with the vertical fluxes neglected). The term $\bar{\boldsymbol{u}}_\mathrm{h}\cdot\boldsymbol{F}_u$ can be decomposed into two parts

$$\bar{\boldsymbol{u}}_\mathrm{h}\cdot\boldsymbol{F}_u = -\overline{\boldsymbol{u}'\boldsymbol{u}'_\mathrm{h}}\cdot\nabla\bar{\boldsymbol{u}}_\mathrm{h} + \nabla\cdot(\bar{\boldsymbol{u}}_\mathrm{h}\cdot\overline{\boldsymbol{u}'\boldsymbol{u}'_\mathrm{h}}) = -\overline{S} + \nabla\cdot(\bar{\boldsymbol{u}}_\mathrm{h}\cdot\overline{\boldsymbol{u}'\boldsymbol{u}'_\mathrm{h}}) \tag{13}$$

in which the first component describes exchange of $\overline{E}$ to $\bar{e}$ and which is identical to the negative of $\overline{S}$, i.e. the energy exchange between MKE and EKE. The second part of $\bar{\boldsymbol{u}}_\mathrm{h}\cdot\boldsymbol{F}_u$ in Eq. (13) is of advective nature and cancels in a volume integral and is therefore usually not interpreted as an energy production term. It is now our aim to derive a parameterized expression for $\boldsymbol{F}_u$ in order to identify the energy production term $\overline{S}$ (and the advective part) in the product $\bar{\boldsymbol{u}}_\mathrm{h}\cdot\boldsymbol{F}_u$ which can then be used in our parameterisation. As noted above, we obtain a parameterisation for $\boldsymbol{F}_u$ by considering potential vorticity mixing.

The quasi-geostrophic potential vorticity,[1] q, is given by

$$q = \nabla_\mathrm{h}^2\Psi + \beta y + \left(\frac{f^2}{N^2}\Psi_z\right)_z \equiv q_\mathrm{r} + q_\mathrm{p} + q_\mathrm{s} \tag{14}$$

where q_r, q_p and q_s denote relative, planetary and stretching vorticity, respectively, and where Ψ denotes the (zero order) geostrophic streamfunction $\boldsymbol{u}_\mathrm{h} = \nabla_\neg\Psi$ with[2] $b = f_0\Psi_z$. By using standard manipulations, it is possible to derive the instantaneous potential vorticity budget

$$\frac{\partial}{\partial t}q + \boldsymbol{u}_\mathrm{h}\cdot\nabla_\mathrm{h}q = \epsilon_q \tag{15}$$

where ϵ_q represents sources and sinks of q. Taking the mean yields

$$\frac{\partial}{\partial t}\bar{q} + \bar{\boldsymbol{u}}_\mathrm{h}\cdot\nabla_\mathrm{h}\bar{q} = -\nabla_\mathrm{h}\cdot\overline{q'\boldsymbol{u}'_\mathrm{h}} + \overline{\epsilon_q} \equiv \nabla_\mathrm{h}\cdot\mathbf{K}_q\nabla_\mathrm{h}\bar{q} + \overline{\epsilon_q} \tag{16}$$

where we have introduced a diffusivity tensor $\mathbf{K}_q$. This tensor describes turbulent diffusion of the mean potential vorticity.

Instead of taking the mean of the instantaneous potential vorticity budget, as discussed above, it is also possible to construct the potential vorticity budget from the mean (first order) momentum and buoyancy budget and continuity equation (in quasi-geostrophic limit), which we consider now. In the mean buoyancy budget, the eddy buoyancy fluxes $\overline{\boldsymbol{u}'_\mathrm{h}b'}$ show up which are expressed as $\overline{\boldsymbol{u}'_\mathrm{h}b'} = -\mathbf{K}\nabla_\mathrm{h}\bar{b}$. Note that we aim to parameterize $\overline{\boldsymbol{u}'_\mathrm{h}b'}$ as before as downgradient diffusion (with a scalar diffusivity $K = \bar{e}^{1/2}L$), but here, however, we have introduced for the moment the diffusivity tensor $\mathbf{K}$ which makes the relation $\overline{\boldsymbol{u}'_\mathrm{h}b'} = -\mathbf{K}\nabla_\mathrm{h}\bar{b}$ exact (by

[1] Note that the QG assumption is applied here for the local eddy dynamics only, while the mean flow might also involve larger scales than those valid within the QG limit.

[2] The operator $\nabla_\neg$ is given by $\nabla_\neg = \left(-\frac{\partial}{\partial y}, \frac{\partial}{\partial x}\right)^\mathrm{T}$, i.e. a shorthand for $\boldsymbol{k}\times\nabla_\mathrm{h}$ (the vector subscript $\neg$ shall denote anti-clockwise rotation of a horizontal vector by 90°).

specifying the components of $\mathbf{K}$ appropriately) in contrast to the previous downgradient parameterisation Eq. (4). In the mean (first order) momentum budget, the eddy momentum fluxes $\boldsymbol{F}_u$ as defined above, show up.

Taking the curl of the mean (first order) momentum equation, using the mean (first order) continuity equation and replacing the vertical derivative of the mean vertical (first order) velocity with the vertical derivative of the mean buoyancy budget, we find

$$\frac{\partial}{\partial t}\bar{q} + \bar{\boldsymbol{u}}_\mathrm{h} \cdot \nabla_\mathrm{h}\bar{q} = \nabla_\mathrm{h} \cdot \mathbf{K}\nabla_\mathrm{h}\bar{q}_\mathrm{s} + \nabla_\mathrm{h} \cdot \mathbf{K}_z\nabla_\mathrm{h}\frac{f^2}{N^2}\overline{\Psi}_z - \stackrel{\nabla}{\neg}\cdot\boldsymbol{F}_u + \overline{\epsilon_q} \tag{17}$$

The term $\nabla_\mathrm{h} \cdot \mathbf{K}\nabla_\mathrm{h}\bar{q}_\mathrm{s} + \nabla_\mathrm{h} \cdot \mathbf{K}_z\nabla_\mathrm{h}\frac{f^2}{N^2}\overline{\Psi}_z$ originates from the vertical derivative of the divergence of the parameterized horizontal eddy buoyancy fluxes $\overline{\boldsymbol{u}'_\mathrm{h}b'} = -\mathbf{K}\nabla_\mathrm{h}\bar{b}$. The term $\stackrel{\nabla}{\neg}\cdot\boldsymbol{F}_u$ in Eq. (17) originates from taking the curl of the mean momentum budget.

We proceed by equating the mean of the instantaneous potential vorticity budget, Eq. (16), and the potential vorticity budget of the mean quantities, Eq. (17), to obtain an expression for $\boldsymbol{F}_u$. To simplify the derivation we first set

$$\boldsymbol{F}_u = -\mathbf{K}_m\stackrel{\nabla}{\neg}(\bar{q}_\mathrm{r} + q_\mathrm{p}) + \mathbf{K}_z\stackrel{\nabla}{\neg}\frac{f^2}{N^2}\bar{\Psi}_z - \nabla_\mathrm{h}\theta \tag{18}$$

introducing, for convenience, another tensor $\mathbf{K}_m$ again by choosing the components of $\mathbf{K}_m$ appropriately. Note that the gauge potential θ drops out in the potential vorticity budget (taking the curl of $\boldsymbol{F}_u$) and is introduced here for later use in Appendix A. The potential vorticity budget of the mean quantities, Eq. (17), then simply becomes

$$\frac{\partial}{\partial t}\bar{q} + \bar{\boldsymbol{u}}_\mathrm{h} \cdot \nabla_\mathrm{h}\bar{q} = \nabla_\mathrm{h} \cdot (\mathbf{K}\nabla_\mathrm{h}\bar{q}_\mathrm{s} + \mathbf{K}_m\nabla_\mathrm{h}(\bar{q}_\mathrm{r} + q_\mathrm{p})) + \overline{\epsilon_q} \tag{19}$$

It is then clear that setting

$$\mathbf{K} \stackrel{!}{=} \mathbf{K}_q \stackrel{!}{=} \mathbf{K}_m \tag{20}$$

yields identical results in Eqs. (16) and (19), i.e. both in the time average of the instantaneous potential vorticity budget and the potential vorticity budget constructed from the mean quantities. In other words, using this setting it is guaranteed that potential vorticity is mixed downgradient (as long as $\mathbf{K}$ is positive definite) and, at the same time, that buoyancy is also mixed (horizontally) downgradient (analogous to the Gent and McWilliams, 1990 parameterisation). Furthermore, the setting implies that the diffusivity (tensor) related to buoyancy and potential vorticity is identical. The consequences of the closure Eqs. (18) and (20) for the mean momentum budget is discussed in Appendix A. It should be noted, however, that the setting Eq. (20) is based on the assumption that different tracers (i.e. potential vorticity and buoyancy) share identical diffusivities which may not be the case.

For simplicity we assume again for our parameterisation that $\mathbf{K} = K$. The energy production term $\overline{S}$ is then finally derived by combining Eq. (13), i.e. the expression for $\boldsymbol{u}_\mathrm{h} \cdot \boldsymbol{F}_u$, with the parameterisation for $\boldsymbol{F}_u$ given by Eq. (18), and with the setting Eq. (20) (with $\mathbf{K} = K$) which yields after some manipulations

$$\begin{aligned}\bar{\boldsymbol{u}}_\mathrm{h} \cdot \boldsymbol{F}_u &= \bar{\boldsymbol{u}}_\mathrm{h} \cdot \left[-K\stackrel{\nabla}{\neg}(\bar{q}_\mathrm{r} + q_\mathrm{p}) + K_z\stackrel{\nabla}{\neg}\frac{f^2}{N^2}\overline{\Psi}_z - \nabla_\mathrm{h}\theta\right] \\ &= (\nabla_\mathrm{h}K) \cdot \nabla_\mathrm{h}E + K|\nabla_\mathrm{h}\boldsymbol{u}_\mathrm{h}|^2 + K_z\frac{f^2}{N^2}\overline{E}_z + \bar{u}\beta K - \nabla_\mathrm{h} \cdot (K\nabla_\mathrm{h}\overline{E} + \boldsymbol{u}_\mathrm{h}\theta)\end{aligned} \tag{21}$$

The last term in brackets on the right hand side of Eq. (21) is similar to the second component in Eq. (13) that is of advective nature, while the remaining terms can finally be identified with $\overline{S}$

$$\overline{S} = K|\nabla_\mathrm{h}\boldsymbol{u}_\mathrm{h}|^2 + \nabla_\mathrm{h}K \cdot \nabla_\mathrm{h}\overline{E} + K_z\frac{f^2}{N^2}\overline{E}_z + \bar{u}\beta K \tag{22}$$

The parameterized energy transfer $\overline{S}$ is decomposed into four parts. The first and second part can be traced back to the diffusion of mean relative vorticity ($\bar{q}_\mathrm{r}$), while the last term on the r.h.s of Eq. (22) is related to the diffusion of mean planetary vorticity ($\bar{q}_\mathrm{p}$). It is shown below that these terms tend to be small, the dominant term is related to the vertical derivative of the thickness diffusivity K, i.e. $f^2 K_z/(N^2 \overline{E}_z)$, which can be traced back to the difference between mixing of mean stretching vorticity ($\bar{q}_s$) and buoyancy.

3.5. The parameterized EKE budget

Collecting now the parameterisations for dissipation, radiation and the energy transfer $\overline{S}$, the EKE budget for the interior ocean ($K_{\rm dia} = 0$) becomes

$$\frac{\partial}{\partial t}\bar{e} + \bar{\boldsymbol{u}} \cdot \nabla \bar{e} = K\tau^2 + (\nabla_{\rm h} K) \cdot \nabla_{\rm h} E + \frac{f^2}{N^2} K_z E_z + \beta K \bar{u} + \nabla_{\rm h} \cdot K \nabla_{\rm h} \bar{e} - \frac{\bar{e}^{3/2}}{L} \tag{23}$$

with the generalized Eady growth rate $\tau^2 = |\nabla_{\rm h} \bar{\boldsymbol{u}}_{\rm h}|^2 + \frac{|\nabla_{\rm h} \bar{b}|^2}{N^2}$. This equation can be prognostically integrated in a coarse resolution model which gives the diffusivity $K = e^{1/2} L$. This diffusivity corresponds to the diffusivity used in the GM parameterisation and is also related to lateral and vertical mixing in the horizontal momentum equations, as discussed in Appendix A.

3.6. Eddy length scale

It is often suggested that the eddy length scale L is given by the local first baroclinic Rossby radius $L_{\rm r}$. However, Rhines (1977) argued[3] that another scale becomes important if the (local) baroclinic Rossby phase speed becomes comparable to the turbulent velocity scale, $U = \bar{e}^{1/2}$, i.e. if

$$U \sim \left| \frac{-\beta}{k^2 + L_{\rm r}^{-2}} \right| \quad \text{or} \quad L^{-2} \sim L_{\rm Rhi}^{-2} + L_{\rm r}^{-2} \tag{24}$$

with the Rhines scale $L_{\rm Rhi} = \sqrt{\frac{U}{\beta}}$ and $L = k^{-1}$. The relation between L, $L_{\rm r}$ and $L_{\rm Rhi}$ in Eq. (24) is numerically almost identical to taking L as the minimum of $L_{\rm Rhi}$ and $L_{\rm r}$. Note that since the restriction of the β-effect does not apply to zonal excursions in the same way as for the meridional excursions, one might use the minimum between $L_{\rm r}$ and $L_{\rm Rhi}$ for the meridional eddy length scale only, while the zonal length scale remains unconstrained by the β effect. In this way, the Rhines scale $L_{\rm Rhi}$ yields a source of anisotropy. We note that such an anisotropy could be implemented as well in our parameterisation, which is, however, not further discussed here.

In many turbulence closures (e.g. Gaspar et al., 1990) it is suggested to use the smallest in case of several competing eddy length scales. In fact, considering effects of Rossby waves on geostrophic turbulence, Eq. (24), suggests to use the minimum of Rossby radius $L_{\rm r}$ and Rhines scale $L_{\rm Rhi}$ consistent with the above argument. Consequently, we choose

$$L = \min(L_{\rm r}, L_{\rm Rhi}) \tag{25}$$

Support for this choice comes from a recent study of Eden (2007). In Eden (2007), eddy length scales in an eddy-resolving model of the North Atlantic and in satellite altimeter data are diagnosed. It was found that north of about 30°N (roughly equivalent to $L_{\rm r} < 30$ km and $L_{\rm r} < L_{\rm Rhi}$), the eddy length scales are indeed proportional to the local Rossby radius $L_{\rm r}$ and that eddy length scales are isotropic. However, south of 30°N (or $L_{\rm r} > 30$ km and $L_{\rm r} > L_{\rm Rhi}$) the turbulent flow becomes anisotropic and eddy length scales are no longer a function of $L_{\rm r}$ but are a function of $L_{\rm Rhi}$. The line separating the isotropic from the anisotropic regime is roughly given by $L_{\rm r} = L_{\rm Rhi}$ (roughly at 30°N). The diagnosis in Eden (2007) thus supports the choice of the eddy length scales in Eq. (25).

Further support for our choice comes from a recent study by Theiss (2004). In an idealised, eddying shallow water model including the latitudinal variation of the Rossby radius (i.e. considering not just a β-plane with fixed Rossby radius as in previous studies), he also found a critical latitude given by $L_{\rm r} = L_{\rm Rhi}$, above which the flow is isotropic and below which the flow becomes anisotropic (zonal scales larger than meridional ones).

[3] Note that Rhines (1977) considered a two-dimensional, barotropic flow. See for a more general discussion, e.g. Theiss (2004) and references therein.

The results by Theiss (2004) are confirmed by numerical experiments in a recent study of Scott and Polvani (in press), to which the reader is referred for a comprehensive review of geostrophic tubulence, including a discussion of Eq. (24). It is also interesting to note that a distinct transition from isotropic turbulence near the poles to anisotropic turbulent flow equatorwards can also be seen in satellite images of jupiter (Theiss, 2006).

3.7. Simplified closures and scaling laws

Neglecting in Eq. (23) the diffusive and advective terms and the energy production term $\overline{S}$ and assuming furthermore $\frac{\partial}{\partial t}\bar{e} = 0$ the following simple expression for EKE, diffusivity K, eddy length scale and time scale are obtained

$$\bar{e}^{1/2} = L\sigma, \quad K = L^2\sigma, \quad L = \min(L_r, \sigma/\beta), \quad \sigma = \frac{f|\boldsymbol{u}_z|}{N} \tag{26}$$

The inverse time scale σ is related to the vertical shear of the mean flow and is identical to the Eady growth rate. In this limit, the closure becomes similar to the parameterisation given in Visbeck et al. (1997). Note, however, that the definition of the length scale L differs from the one in Visbeck et al. (1997). Note also that the scaling in Eq. (26) for EKE and diffusivity is identical to the scaling in Larichev and Held (1995) and Held and Larichev (1996) for isotropic homogeneous turbulence of baroclinic quasi-geostrophic flow. This means that the non-local budget given by Eq. (23) can be viewed as the extension of the closure for homogeneous isotropic quasi-geostrophic turbulence (Eq. (26)) to the inhomogeneous and anisotropic case, which might be more relevant to the ocean.

4. Numerical experiments

4.1. Eddy-resolving models

We use two realistic eddy-resolving models to evaluate the turbulence closure. The first covers the North Atlantic with horizontal resolution of about 10 km at the equator decreasing to about 5 km in high latitudes. The model domain extends from 20°S to 70°N with open boundaries (Stevens, 1990) at the northern and southern boundaries and with a restoring zone in the eastern Mediterranean Sea. There are 45 vertical geopotential levels with increasing thickness with depth, ranging from 10 m at the surface to 250 m near the maximal depth of 5500 m. The model is based on a rewritten version[4] of MOM2 (Pacanowski, 1995) and is identical to the one used in Eden (2007). All moments shown here are averaged over 5 years following a spin-up phase of 10 year model integration using climatological monthly mean surface forcing.

A second eddy-resolving model is used to assess the validity of the turbulence model in the Southern Ocean. The horizontal resolution of this model is 1/10° with 42 vertical levels ranging from 10 m at the surface to 250 m at depth. The model domain covers the latitudinal belt between 78°S and 30°S with open boundaries at 30°S. The model is based on the same code as the North Atlantic model and identical to the one used in Eden (2006). The model is forced with similar monthly mean climatological forcing as the North Atlantic model for a spin-up phase of 10 years, after which in a 5-year analysis period moments of eddy fluxes are averaged. Sub-grid-scale parameterisations are similar as in the North Atlantic model, except for slightly higher biharmonic diffusivity and viscosity of 0.8×10^{10} m^4/s and 2×10^{10} m^4/s, respectively.

4.2. Testing eddy length scale and mixing length assumption

The diffusivity $K = \bar{e}^{1/2}L$ using the EKE, $\bar{e}$, as simulated by the models and using different length scales L are compared with independent direct estimates of the thickness diffusivity (K_{est}) from the model results. In Eden et al. (2007b) and Eden (2006), the eddy buoyancy flux $\overline{\boldsymbol{u}'b'}$ is diagnosed in the eddy-resolving models from which a diffusivity K_{est} is estimated. It is shown in Eden et al. (2007b) that the fluxes $\overline{\boldsymbol{u}'b'}$ have to be decomposed into a rotational and remaining part, which can be done in different ways giving slightly different

[4] The numerical code together with all configurations used in this study can be accessed at http://www.ifm-geomar.de/~spflame.

results. Moreover, the estimated diffusivities often tend to get negative which cannot be modelled in a turbulence closure based on a mixing length assumption Eq. (5). However, the diffusivity K_{est} estimated as in Eden et al. (2007b) and Eden (2006) should give the magnitude and pattern of the "real" diffusivity, is physically plausible, and can be compared with the parameterisation of K.

Fig. 1a shows K_{est} in the North Atlantic at 300 m depth. Magnitudes range from zero to 5000 m^2/s and whereas K_{est} is mostly positive away from the equatorial regions, it tends to become negative in regions with large EKE. Fig. 1b shows $K = e^{1/2}L_{\mathrm{r}}$. The Rossby radius L_{r} was estimated from $L_{\mathrm{r}} = \min\left[\frac{c_{\mathrm{r}}}{|f|}, \sqrt{\frac{c_{\mathrm{r}}}{2\beta}}\right]$ where c_{r} denotes the first baroclinic Rossby wave speed, f the Coriolis parameter and $\beta = \frac{\partial f}{\partial y}$. The Rossby wave speed c_{r} was calculated from the local mean stratification approximately following Chelton et al. (1998) by $c_{\mathrm{r}} \approx \int_{-h}^{0} N/\pi \, \mathrm{d}z$, where h denotes the local water depth.

$K = e^{1/2}L_{\mathrm{r}}$ appears to be too large near the equator (values reach more than 20×10^3 m^2/s). On the other hand, it appears that $K = e^{1/2}L_{\mathrm{r}}$ and K_{est} are similar over wide regions of the subpolar North Atlantic. Fig. 1c shows the diffusivity $K = e^{1/2}L_{\mathrm{Rhi}}$, where L_{Rhi} is the Rhines scale. It is much smaller in the subtropical and

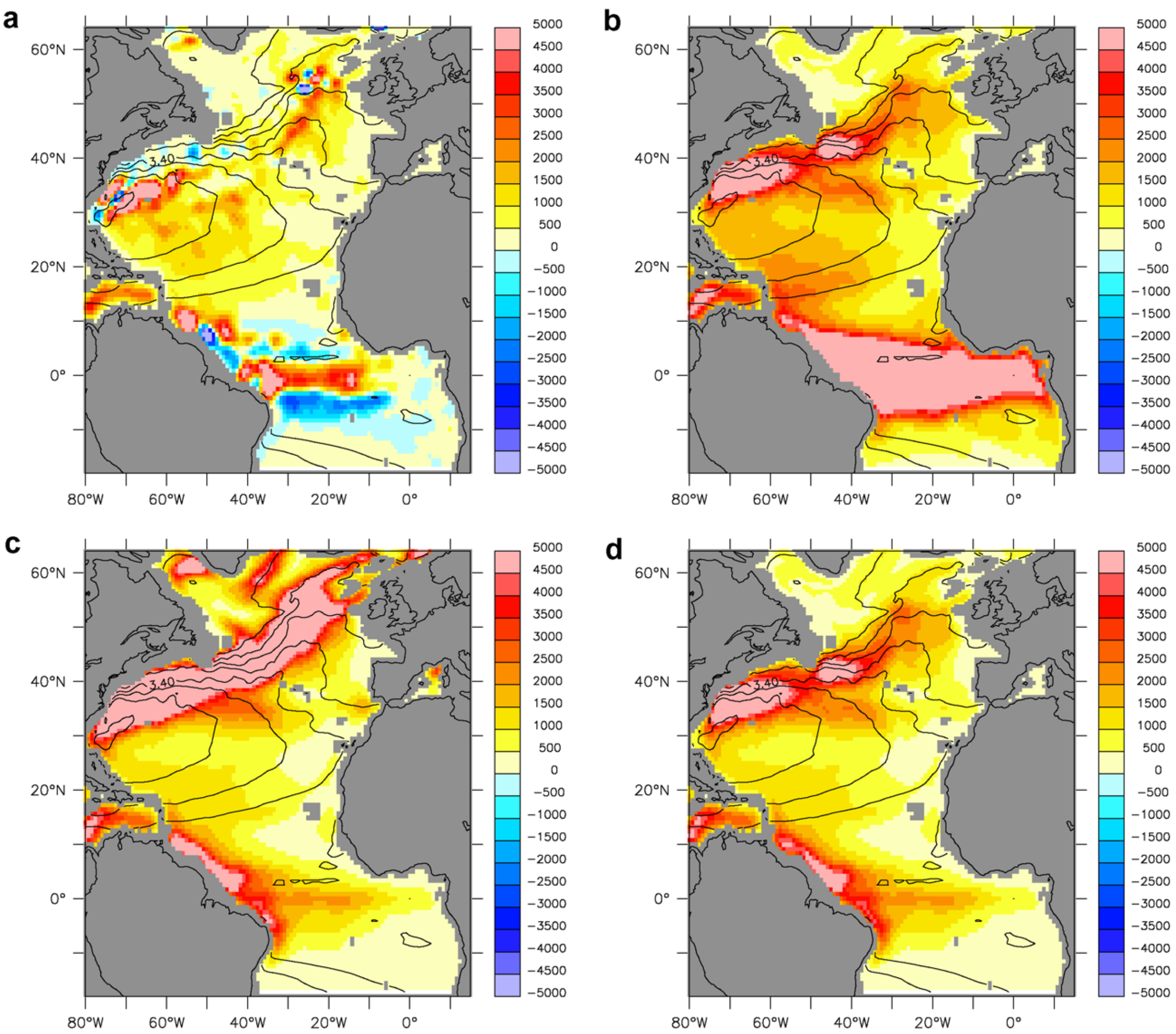

Fig. 1. (a) K_{est} at 300 m depth in the North Atlantic in m^2/s. (b) Same as (a) but $K = e^{1/2}L_{\mathrm{r}}$, (c) $K = e^{1/2}L_{\mathrm{Rhi}}$ and (d) $K = e^{1/2}\min(L_{\mathrm{r}}, L_{\mathrm{Rhi}})$. Also shown are mean density contours (solid lines).

tropical North Atlantic than $K = e^{1/2}L_r$, and reaches similar values to K_{est} in the subtropics and tropics. However, larger values of $K = e^{1/2}L_{Rhi}$ than K_{est} show up in the subpolar North Atlantic. It is evident from the figures that L_r is the best choice for the eddy length scale in the subpolar North Atlantic, while L_{Rhi} should be chosen for the subtropical and tropical North Atlantic. Fig. 1d shows the diffusivity using the minimum of L_r and L_{Rhi} (Eq. (25)). It is indeed evident that the choice given by Eq. (25) agrees with K_{est} best.

Fig. 2 shows the corresponding results for the Southern Ocean. Clearly, K_{est} is smaller here compared to the North Atlantic over large regions; only equatorwards of the ACC, the values of K_{est} exceed 2000 m^2/s. The zonal average of K_{est} shows, similar to the North Atlantic (not shown), decaying values of K_{est} below the thermocline. Both the large scale horizontal pattern and vertical dependency of K_{est} can be reproduced with $K = e^{1/2}L_r$ while $K = e^{1/2}L_{Rhi}$ shows too large values. Overall, the results from the model of the Southern Ocean are in good agreement to the results from the subpolar North Atlantic.

4.3. Application of the closure in coarse resolution models

We proceed to test the closure in non-eddy resolving models of the North Atlantic and the Southern Ocean. Both models are coarse resolution versions of the above discussed eddy-resolving models, i.e. with 4/3° and 1° horizontal resolution in the North Atlantic and the Southern Ocean, respectively. Surface forcing and lateral

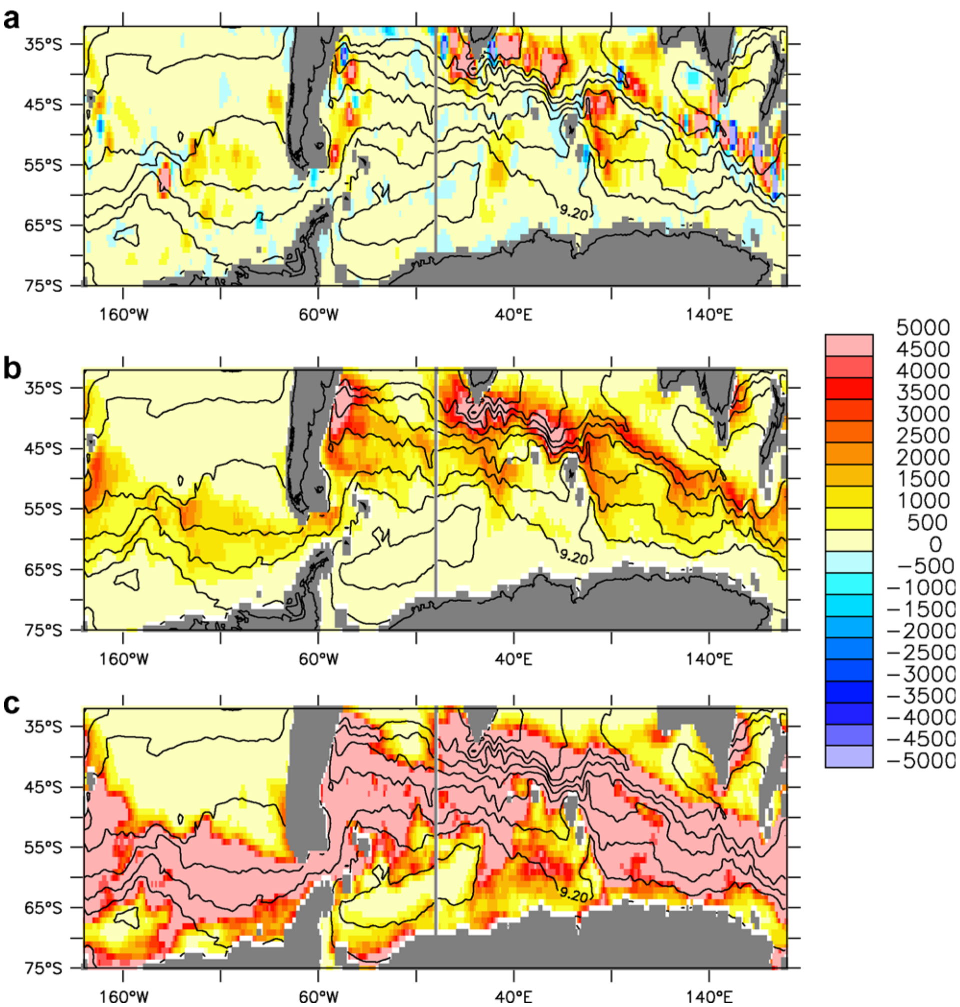

Fig. 2. (a) Shows K_{est} in the Southern Ocean in m^2/s, (b) $K = e^{1/2}L_r$ and (c) $K = e^{1/2}L_{Rhi}$ at 300 m depth. Also shown are mean density contours (solid lines).

boundary conditions are identical to the high resolution cases, except for closed (instead of open) boundaries in the North Atlantic model (where simple restoring zones replace the open boundary conditions). The North Atlantic model is very similar to the one used in e.g. Eden and Greatbatch (2003). Results are shown after 20 years of integration.

We have integrated the EKE budget according to

$$\frac{\mathrm{d}}{\mathrm{d}t}\bar{e} = K|\nabla_\mathrm{h}\bar{\boldsymbol{u}}_\mathrm{h}|^2 + K\frac{|\nabla_\mathrm{h}\bar{b}|^2}{N^2} + \frac{f^2}{N^2}K_z E_z + \nabla_\mathrm{h}\cdot K\nabla_\mathrm{h}\bar{e} + \left(K\frac{0.1f^2}{N^2}\bar{e}_z\right)_z - c_\epsilon\frac{\bar{e}^{3/2}}{L} \tag{27}$$

in the coarse models and have replaced the thickness diffusivity in the models by $K = \bar{e}^{1/2}L$ (vertical and horizontal viscosity in the momentum equation together with the isopycnal diffusivity was left unchanged in the model simulation). The closure in Eq. (23) was modified by neglecting the terms $\beta K u$ and $\nabla_\mathrm{h}K\cdot\nabla\overline{E}$, which are both small compared to the other production terms as inferred from the eddy-resolving models (not shown), although the former can become significant near the equator. However, we have decided to neglect the term related to β for now, which can be justified since for the local eddy dynamics the planetary vorticity change

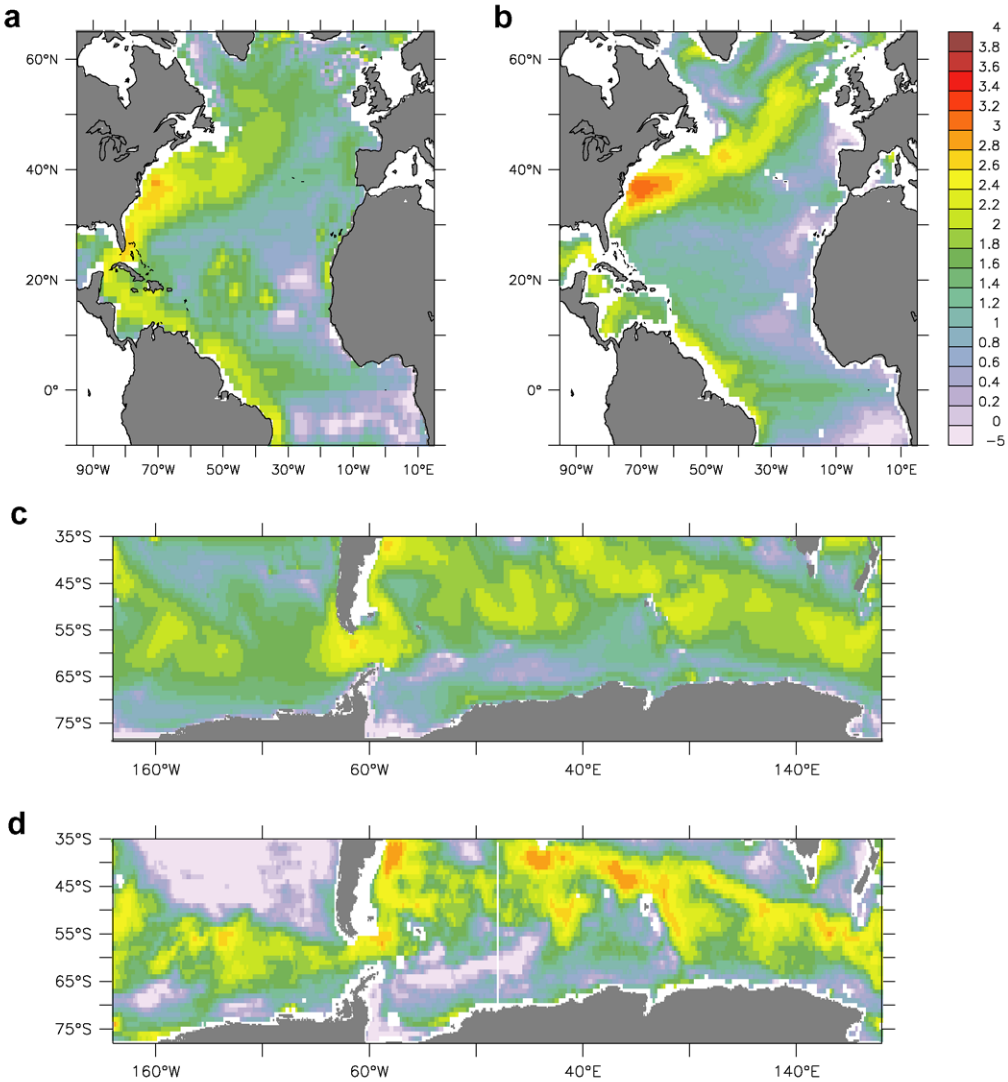

Fig. 3. Logarithm of parameterized EKE in the coarse resolution model (a, c) and the EKE in the eddy-resolving model (b, d) at 300 m depth in $\log_{10}(\bar{e}/[\mathrm{cm}^2/\mathrm{s}^2])$.

does not contribute much to the potential vorticity budget, since eddies transfer properties (including planetary vorticity) only over short distances. We have also introduced vertical mixing of EKE using $0.1\frac{f^2}{N^2}K$ as vertical diffusivity and an additional parameter c_ϵ, scaling the dissipation in the EKE budget. The length scale L was chosen as

$$L = \min[2L_\mathrm{r}, 0.3L_\mathrm{Rhi}] \tag{28}$$

with $L_\mathrm{r} = \min\left[\frac{c_\mathrm{r}}{|f|}, \sqrt{\frac{c_\mathrm{r}}{2\beta}}\right]$ and $L_\mathrm{Rhi} = \sqrt{\frac{\bar{e}^{1/2}}{\beta}}$. It is clear that we have chosen all parameters to come close to the results of the eddy resolving models (although it should be noted that the same modifications are used in both models, providing a test in two different flow regimes for the non-eddy resolving resolution of order 1 degree longitude used here). Most important is the parameter c_ϵ since it determines to a large extent the level of EKE in the closure. Since we found it necessary to choose c_ϵ significantly smaller than one, i.e. $c_\epsilon = 0.1$, it appears that an appropriate dissipation length scale is larger than the eddy length scale. This is consistent with direct estimates of the dissipation by biharmonic friction in the eddy-resolving models (not shown). It was also found necessary to further increase the length scale in the isotropic mixing regime (where L_r sets the length scale) and to decrease it in the non-isotropic mixing regime near the equator. The line separating both regions is therefore shifted by about 10° latitude to the north compared to the results in Eden (2007).

To prevent a singularity, we have tapered the production terms $K\frac{|\nabla_\mathrm{h}\bar{b}|^2}{N^2}$ and $\frac{f^2}{N^2}K_zE_z$ to zero for $N \to 0$. In such regions, represented essentially by the surface mixed layer but also by some grid points in the abyssal ocean, additional lateral diffusion with diffusivity K was applied to the tracers as originally proposed by Treguier et al. (1997) in order to account for the impact of non-zero K_dia (see Eq. (8) and the brief discussion in Section 5). A vertical transition zone from the stratified interior to regions where $N \to 0$ of one vertical grid box was used. We found the results rather sensitive to the choice of such a transition zone as also discussed

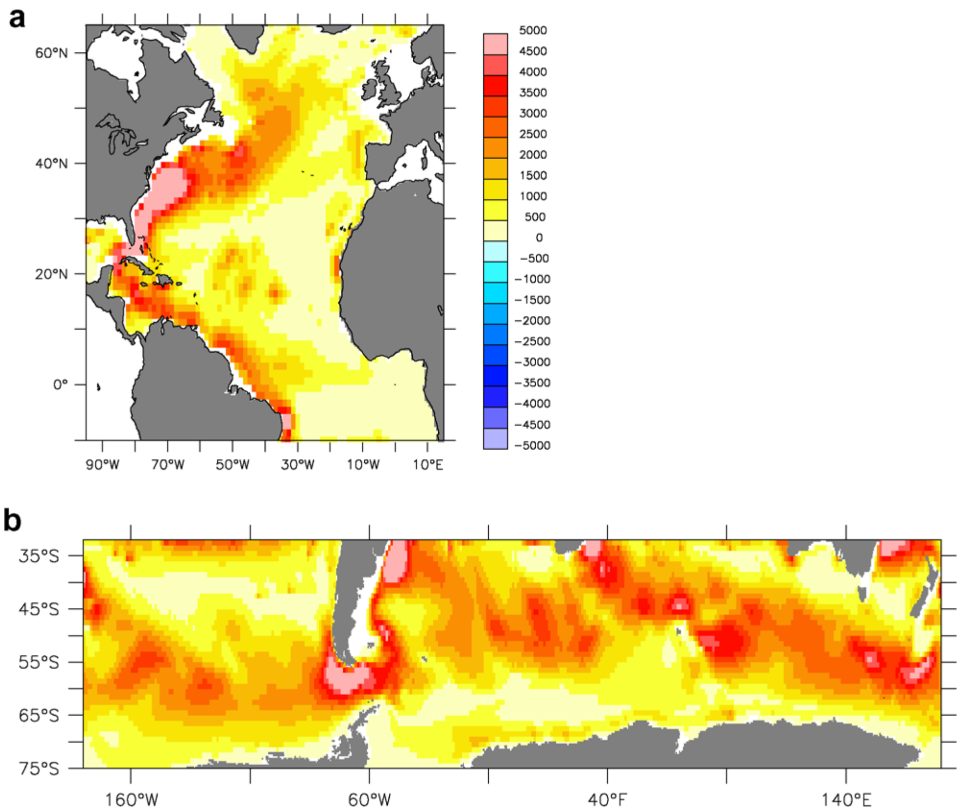

Fig. 4. Parameterized K in the coarse resolution model at 300 m depth in m^2/s in the North Atlantic (a) and the Southern Ocean (b).

recently by Danabasoglu et al. (submitted for publication). Since the baroclinic instability production terms $K\frac{|\nabla_h \bar{b}|^2}{N^2}$ and $\frac{f^2}{N^2}K_z E_z$ become zero in the surface mixed layer, it appears that the closure lacks sufficient EKE production in the isotropic mixing regime where mixed layers are deeper compared to the subtropics and tropics. Consequently, we found it necessary to increase the eddy length scale in the northern North Atlantic. The lack of baroclinic instability production terms is thus identified as a drawback of the current closure.

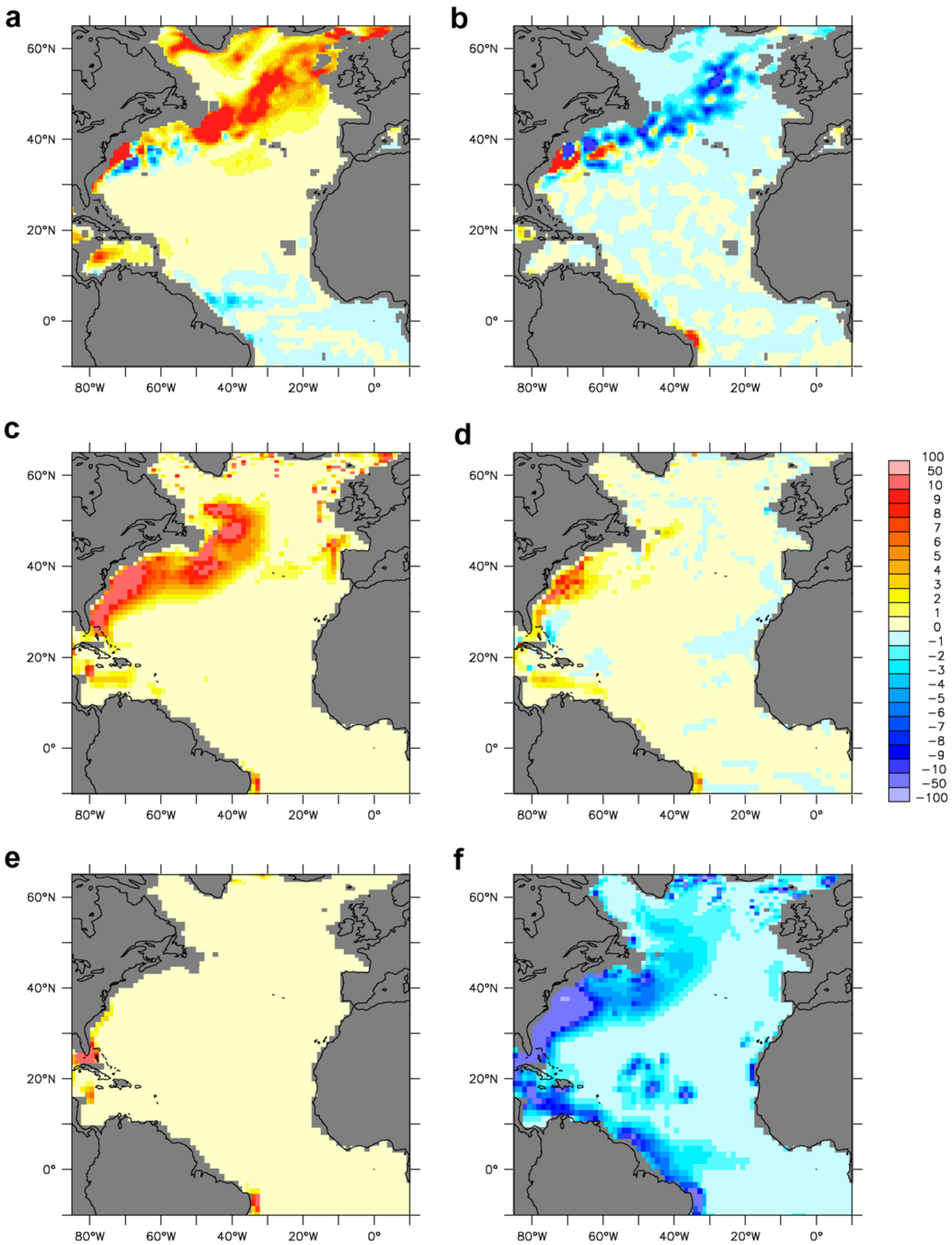

Fig. 5. (a) Energy transfer $\overline{b'w'}$ diagnosed from the eddy resolving model at 300 m depth in 10^{-9} m^2/s^3. Data are computed from seasonal means over 5 years and are spatially averaged over 15 grid points. (b) Same as (a) but energy transfer $\overline{S}$. (c) Annual mean energy production term $K|\nabla_h \bar{b}|^2/N^2$ in the coarse resolution model at 300 m depth in 10^{-9} m^2/s^3. (d) Same as (c) but the term $f^2K_z/(E_zN^2)$. (e) Same as (c) but the term $K|\nabla_h \boldsymbol{u}_h|^2$. (f) Same as (c) but the term $c_\epsilon \bar{e}^{3/2}/L$.

The results of this first application of the simple eddy closure in terms of EKE and K are, however, remarkably close to the eddy resolving models. Fig. 3 shows the simulated EKE distribution in the coarse resolution model and the eddy-resolving model at 300 m depth both for the North Atlantic and the Southern Ocean. The pattern and amplitude of EKE simulated by the eddy-resolving models is well reproduced by the parameterisation, only a small bias towards too high levels of EKE can be found near the eastern equatorial Atlantic and a small bias towards too low levels can be found north of the subpolar front in both Atlantic and Southern Ocean. Note that the bias towards too low levels in the high latitudes is related to the missing baroclinic instability production term in the deeper mixed layers at high latitudes, as discussed above. Results at other depth levels are similarly convincing, although a bias towards too low values in the deep equatorial ocean can be found, which might be related to the focus on quasi-geostrophic dynamics in the present parameterisation.

Given the successful simulation of the EKE, it is not surprising that the resulting diffusivities in the coarse resolution model fit the analysis of the eddy-resolving models as well. Fig. 4 shows K at 300 m depth on the same colour scale as in Figs. 1 and 2. Clearly the pattern of the simulated $K = \bar{e}^{1/2}L$ from the eddy resolving model corresponds well to the parameterisation. This holds also at other depth levels (not shown).

A comparison of the individual energy production rates in the parameterisation with the respective quantities in the eddy-resolving model is shown in Fig. 5 at 300 m depth for the North Atlantic. The energy production due to baroclinic instability (Fig. 5a) is large in the Gulf Stream/North Atlantic Current system and in the subpolar North Atlantic. The parameterized term $K|\nabla_h \bar{b}|^2/N^2$ (Fig. 5c) shows in general good agreement with $\overline{b'w'}$ with respect to its pattern and amplitude. The largest difference is given by a bias towards too low values in the subpolar North Atlantic, as already discussed above. Another difference are negative values of $\overline{b'w'}$ in the Gulf Stream region and in the tropical Atlantic Ocean. In these regions, negative K are found by Eden et al. (2007b), diagnosing K from the eddy-resolving model. Note that negative values of K in the parameterized term $K|\nabla_h \bar{b}|^2/N^2$ cannot be reproduced with the mixing length closure Eq. (5), pointing towards a principle limitation of the closure.

The energy production related to eddy momentum fluxes, $\overline{S}$ (Fig. 5b), is of similar magnitude as $\overline{b'w'}$ and shows also negative values-here downstream of the Gulf Stream- and predominantly positive values within the Gulf Stream region. Again, the negative values are not reproduced by the parameterisation. The dominant term in the parameterized version of $\overline{S}$ is given by $f^2K_z/(E_zN^2)$ (Fig. 5d), while the term related to the shear of the mean flow, $K|\nabla_h \boldsymbol{u}_h|^2$ (Fig. 5e), is neglegible. The term $f^2K_z/(E_zN^2)$ has a maximum in the Gulf Stream region, consistent with the estimated $\overline{S}$ in the eddy resolving model, but shows almost no negative values downstream, resembling a further drawback of the parameterisation.

5. Conclusions and discussion

A simple three-dimensional turbulence closure for the effect of mesoscale eddies in realistic ocean models was presented. The closure is given by a prognostic equation for EKE, Eq. (23), from which, together with a diagnostic equation for the eddy length scale, Eq. (25), a diffusivity K can be calculated using the mixing length assumption Eq. (5). The (three-dimensional) EKE equation can be integrated prognostically in a non-eddy-resolving model, simply as an additional tracer. The diffusivity K is related to isopycnal thickness diffusivity of the GM parameterisation, i.e. it gives the eddy-induced velocity which, together with the mean velocity, advects (mean) tracer in an ocean climate model. Furthermore it is outlined in Appendix A how the diffusivity K can be related to horizontal and vertical mixing in the momentum equation.

Using two eddy-resolving models of the North Atlantic and the Southern Ocean, and their non-eddy-resolving counterparts, the performance of the closure was evaluated. It was shown that the classical mixing length assumption together with the definition of the eddy length scale yields good results in terms of diffusivity in both eddy-resolving models when compared to independent estimates of Eden et al. (2007b) and Eden (2006). Further support for the definition of the length scale, comes from an independent estimation of eddy length scales by Eden (2007). Anisotropic lateral mixing indicates the importance of the Rhines scale, in the subtropical and tropical North Atlantic, while the Rossby radius was found to be the relevant eddy length scale in higher latitudes. This is in agreement to idealized numerical experiments by Theiss (2004) and Scott and Polvani (in press). It is thus concluded that using the mixing length assumption of Green (1970) and Stone

(1972), as formulated for the diffusivity (corresponding to the thickness diffusivity in the GM parameterisation) appears to be valid, within certain limitations, as discussed below.

A first application of the closure in the non-eddy-resolving model proves to be successful in terms of reproducing the simulated EKE and diffusivity, when compared to the eddy-resolving models. A bias in the parameterisation is given by a lack of EKE production due to baroclinic instability near and in the surface mixed layer in the subpolar regions. This bias is related to a singularity of the closure for $N \rightarrow 0$ caused by the assumption of zero diapycnal eddy fluxes ($K_{\mathrm{dia}} = 0$), pointing towards the need of a relaxation of this assumption. Another drawback of the parameterisation is the inability of the mixing length assumption to yield negative diffusivities. We found regions of negative values of EKE production due to baroclinic instability, $\overline{b'w'}$, in the Gulf Stream region and the tropical Atlantic Ocean, coming along with negative K as diagnosed from the eddy-resolving model (Eden et al., 2007b). A negative K would thus also be needed in the parameterized version of $\overline{b'w'}$, i.e. in $K|\nabla_{\mathrm{h}}\bar{b}|^2/N^2$, to reproduce the results of the eddy resolving model, pointing towards a principle restriction of the mixing length approach.

We have implemented identical (scalar) diffusivities for potential vorticity ($\bar{q}$) and buoyancy ($\bar{b}$) to construct a parameterisation for the EKE production related to eddy momentum fluxes, $\overline{S}$, given essentially by $\overline{S} \approx f^2 K_z/(E_z N^2)$. As before for the production term $\overline{b'w'}$, negative values of $\overline{S}$ in the eddy resolving model are not well reproduced by the parameterised version of $\overline{S}$. Note that this term is only negative (for $K > 0$) if either the thickness diffusivity K or the mean kinetic energy $\overline{E}$ increases with depth, while the other quantity decreases with depth. On the other hand, the diagnosis in Eden et al. (2007b) and Eden (2006) demonstrates that K in general decreases with depth, which is certainly also true for $\overline{E}$ almost everywhere in the worlds ocean. The reason for the failure of the closure to produce negative values might thus be related to our assumption of identical diffusivities for $\bar{q}$ and $\bar{b}$ and will be investigated in a future study. We also note that the neglection of the parameterized term $\overline{S}$ would in principle produce the same results in terms of simulated EKE as discussed here.

However, despite its principle limitations, the new parameterisation certainly yields good results in terms of the simulated EKE and K. Note also that the application of the identical parameterisation yields similarly good results in the different dynamical regimes, i.e. the North Atlantic and the Southern Ocean. On the other hand, the implementation of a more realistic pattern of diffusivity does not change the simulation of the mean quantities much in both coarse resolution models (not shown). Mean transports and mean buoyancy distributions are almost unchanged comparing model experiments with fixed, spatially uniform values for the thickness diffusivity and the spatially varying diffusivities as given by the present parameterisation. However, first tests using K as isopycnal diffusivity show large sensitivity of the simulation of biogeochemical tracers to the spatial dependency of K.

It was argued when discussing Eq. (8) that the diffusivity, K, should be set equal to the eddy-induced diapycnal diffusivity, K_{dia}, in the surface mixed layer. Zhai and Greatbatch (2006a) have made a first attempt to evaluate K_{dia} from satellite data and Zhai and Greatbatch (2006b) and Greatbatch et al. (2007) have argued that K_{dia} is strongly influenced by the interaction between the eddies and the atmosphere, especially through the surface heat flux (see also Tandon and Garrett, 1996) issues that require exploring further in the context of how to parameterise K_{dia} for use in non-eddy-resolving models.

Acknowledgements

This study was supported by the Deutsche Forschungsgemeinschaft within the SPP 1158. The eddy-resolving model integrations have been performed on a NEC-SX8 at the computing centre at the University Kiel, Germany and on a NEC-SX6 at the Deutsches Klimarechenzentrum (DKRZ), Hamburg, Germany. R.J.G. is grateful for support from the NSERC Discovery Grant program and the NSERC/MARTEC/MSC Industrial Research Chair.

Appendix A. Residual momentum budget

In this section, we explore the consequences of the parameterisation for the eddy momentum fluxes, Eq. (18), on the averaged momentum budget. We work in the Transformed Eulerian Mean (TEM) framework of Andrews and McIntyre (1976), but note that similar results are also obtained for the Eulerian mean momentum budget. We will show how the diffusivity K is related to horizontal and vertical mixing.

Following TEM it is possible to define a residual velocity $\boldsymbol{u}^*$ as

$$\boldsymbol{u}^* = \bar{\boldsymbol{u}} + \nabla \times \boldsymbol{B} \tag{29}$$

The momentum budget formulated for the residual velocity can be written within the quasi-geostrophic approximation as

$$\frac{\partial}{\partial t}\boldsymbol{u}_{\mathrm{h}}^* + \boldsymbol{u}^* \cdot \nabla \boldsymbol{u}_{\mathrm{h}}^* + f\boldsymbol{k} \times \boldsymbol{u}^* = -\nabla_{\mathrm{h}}\bar{p} - \boldsymbol{F}_u + f(K \overset{\nabla}{\neg} \bar{b}N^{-2})_z \tag{30}$$

Note that some terms involving the Eulerian mean velocity $\bar{\boldsymbol{u}}_{\mathrm{h}}$ in the residual momentum equation have been replaced here with $\boldsymbol{u}_{\mathrm{h}}^*$, in accordance to quasi-geostrophic scaling (Plumb and Ferrari, 2005). Note also that the term $-\boldsymbol{F}_u + f(K \overset{\nabla}{\neg} \bar{b}N^{-2})_z$ takes the same meaning as the divergence of the Eliassen–Palm flux in the TEM framework (Andrews et al., 1987), and that the term $f(K \overset{\nabla}{\neg} \bar{b}N^{-2})_z = \left(K \frac{f^2}{N^2}(\bar{\boldsymbol{u}}_{\mathrm{h}})_z\right)_z$ acts as vertical friction (Greatbatch and Lamb, 1990). Using the parameterisation Eq. (18) for $\boldsymbol{F}_u$ in Eq. (30) gives after some manipulations

$$\frac{\partial}{\partial t}\boldsymbol{u}_{\mathrm{h}}^* + \boldsymbol{u}^* \cdot \nabla \boldsymbol{u}_{\mathrm{h}}^* + f\boldsymbol{k} \times \boldsymbol{u}^* = -\nabla_{\mathrm{h}}\bar{p} + K\nabla_{\mathrm{h}}^2\bar{\boldsymbol{u}}_{\mathrm{h}}^* + K\left(\frac{f^2}{N^2}(\boldsymbol{u}_{\mathrm{h}}^*)_z\right)_z - \beta K\boldsymbol{i} + \nabla\theta \tag{31}$$

Note that again some terms involving $\bar{\boldsymbol{u}}_{\mathrm{h}}$ have been replaced here by $\boldsymbol{u}_{\mathrm{h}}^*$. The parameterized eddy effect is given by two forces akin to horizontal and vertical mixing of momentum, a force related to the planetary vorticity gradient and a force related to the gauge function. Horizontal viscosity is the same as the diffusivity, K, while the vertical viscosity is a scaled diffusivity. It should also be noted that the viscosities appear outside the derivatives. The term $-\beta K\boldsymbol{i}$ originating from implementing potential vorticity mixing is related to the additional eddy-driven tracer advection velocity related to β as discussed by e.g. Killworth (1997) and Treguier et al. (1997).

Note that there is an integral constraint on the eddy forces in the momentum budget (see Marshall, 1981). Since eddies only redistribute momentum the volume integrated eddy force should vanish. This integral constraint complicates the implementation of PV mixing in ocean models. However, it is certainly possible to choose the gauge potential θ such that

$$\int \left(-K\nabla_{\mathrm{h}}^2\bar{u}_{\mathrm{h}}^* - K\left(\frac{f^2}{N^2}(u_{\mathrm{h}}^*)_z\right)_z + \beta K\right)\mathrm{d}V = \int \theta_x \, \mathrm{d}V \tag{32}$$

and similar for the meridional momentum. Specifying for instance $\theta = ax + by$ gives parameters a and b which can be chosen to satisfy the two integral constraints.

References

Andrews, D.G., Holton, J.R., Leovy, C.B., 1987. Middle Atmosphere Dynamics. Academic Press.

Andrews, D.G., McIntyre, M.E., 1976. Planetary waves in horizontal and vertical shear: The generalized Eliassen-Palm relation and the zonal mean accelaration. J. Atmos. Sci. 33, 2031–2048.

Canuto, V.M., Dubovikov, M.S., 2006. Dynamical model of mesoscales in z-coordinates. Ocean Modell. 11, 123–166.

Canuto, V.M., Dubovikov, M.S., 2007. Reply to the comment by T.J. McDougall, P.R. Gent and S. Drijfhout. Ocean Modell. 17 (2), 172–181.

Chelton, D.B., deSzoeke, R.A., Schlax, M.G., Naggar, K.E., Siwertz, N., 1998. Geographical variability of the first-baroclinic rossby radius of deformation. J. Phys. Oceanogr. 28, 433–460.

Danabasoglu, G., Ferrari, R., McWilliams, J.C., submitted for publication. Sensitivity of an ocean general circulation model to a parameterization of near-surface eddy fluxes. J. Climate.

Danabasoglu, G., Marshall, J., 2007. Effects of vertical variations of thickness diffusivity in an ocean general circulation model. Ocean Modell. 18, 122–141. doi:10.1016/j.ocemod.2007.03.006.

Eden, C., 2006. Thickness diffusivity in the Antarctic Circumpolar Current. Geophys. Res. Lett. 33 (L11606). doi:10.1029/2006GL026157.

Eden, C., 2007. Eddy length scales in the North Atlantic. J. Geophys. Res. 112 (C06004). doi:10.1029/2006JC003901.

Eden, C., Greatbatch, R.J., 2003. A damped decadal oscillation in the North Atlantic climate system. J. Climate 16, 4043–4060.

Eden, C., Greatbatch, R.J., Olbers, D., 2007a. Interpreting eddy fluxes. J. Phys. Oceanogr. 37, 1282–1296.

Eden, C., Greatbatch, R.J., Willebrand, J., 2007b. A diagnosis of thickness fluxes in an eddy-resolving model. J. Phys. Oceanogr. 37, 727–742.

Ferreira, D., Marshall, J., Heimbach, P., 2005. Estimating eddy stresses by fitting dynamics to observations using a residual-mean ocean circulation model and its adjoint. J. Phys. Oceanogr. 35, 1891–1910.

Gaspar, P., Gregoris, Y., Lefevre, J.-M., 1990. A simple eddy kinetic energy model for simulations of the oceanic vertical mixing: tests at station PAPA and Long-Term Upper Ocean Study site. J. Geophys. Res. 95, 16179–16193.

Gent, P.R., McWilliams, J.C., 1990. Isopycnal mixing in ocean circulation models. J. Phys. Oceanogr. 20, 150–155.

Gent, P.R., Willebrand, J., McDougall, T.J., McWilliams, J.C., 1995. Parameterizing eddy-induced tracer transports in ocean circulation models. J. Phys. Oceanogr. 25, 463–474.

Gnanadesikan, A., Dixon, K.W., Griffies, S.M., Delworth, T.L., Harrison, M.J., Held, I.M., Hurlin, W.J., Pacanowski, Rosati, Samuels, Spelman, Stouffer, Winton, Wittenberg, Dunne, 2006. GFDL's CM2 global coupled climate models. Part II: The baseline ocean simulation. J. Climate 19, 675–697.

Greatbatch, R.J., Lamb, K., 1990. On parameterizing vertical mixing of momentum in non-eddy-resolving ocean models. J. Phys. Oceanogr. 20, 1634–1637.

Greatbatch, R.J., Zhai, X., Eden, C., Olbers, D., 2007. The possible role in the ocean heat budget of eddy-induced mixing due to air-sea interaction. Geophys. Res. Lett. 34 (L07604). doi:10.1029/2007GL029533.

Green, J.S., 1970. Transfer properties of the large-scale eddies and the general circulation of the atmosphere. Quart. J. Roy. Meteor. Soc. 96, 157–185.

Held, I., Larichev, V., 1996. A scaling theory for horizontally homogeneous, baroclincally unstable flow on a beta plane. J. Atmos. Sci. 53 (7), 946–952.

Killworth, P.D., 1997. On the parameterization of eddy transfer. Part I. Theory. J. Mar. Res. 55, 1171–1197.

Larichev, V., Held, I., 1995. Eddy amplitudes and fluxes in a homogenous model of fully developed baroclinic instability. J. Phys. Oceanogr. 25, 2285–2297.

Marshall, J.C., 1981. On the parameterization of geostrophic eddies in the ocean. J. Phys. Oceanogr. 11, 1257–1271.

McDougall, T., Gent, P., Drijfhout, S., 2007. Comment on Dynamical model of mesoscales in z-coordinates and The effect of mesoscales on the tracer equation in z-coordinates OGCMs by VM Canuto and MS Dubovikov. Ocean Modell. 17 (2), 163–171.

McDougall, T.J., McIntosh, P.C., 2001. The temporal-residual-mean velocity. Part II: Isopycnal interpretation and the tracer and momentum equations. J. Phys. Oceanogr. 31 (5), 1222–1246.

Mellor, G.L., Yamada, L., 1982. Development of a turbulence closure model for geophysical fluid problems. Rev. Geophys. 20, 851–875.

Pacanowski, R.C., 1995. MOM 2 documentation, User's guide and reference manual. Technical Report, GFDL Ocean Group, GFDL, Princeton, USA.

Plumb, R.A., Ferrari, R., 2005. Transformed eulerian-mean theory. Part I: Nonquasigeostrophic theory for eddies on a zonal-mean flow. J. Phys. Oceanogr. 35 (2), 165–174.

Prandtl, L., 1925. Bericht über Untersuchungen zur ausgebildeten Turbulenz. Zeitschrift für angewandte Mathematik und Mechanik 5 (2), 136–139.

Rhines, P., 1977. The Dynamics of Unsteady Currents. In: The Sea, vol. 6. Wiley, New York, pp. 189–318.

Rodi, W., 1980. Turbulence models and their applications in hydraulics. Technical Report, Int. Assoc. for Hydraul. Res., Delft, Netherlands.

Salmon, R., 1998. Lectures on Geophysical Fluid Dynamics. Oxford University Press, Oxford.

Schlösser, F., Eden, C., 2007. Diagnosing the energy cascade in a model of the North Atlantic. Geophys. Res. Lett. 34 (L02604). doi:10.1029/2006gl027813.

Scott, R.B., Wang, F., 2005. Direct evidence of an oceanic inverse kinetic energy cascade from satellite altimetry. J. Phys. Oceanogr. 35, 1650–1666.

Scott, R.K., Polvani, L.M., in press. Forced dissipative shallow water turbulence on the sphere: equatorial confinement of zonal jets. J. Atmos. Sci.

Stevens, D.P., 1990. On open boundary conditions for three dimensional primitive equation ocean circulation models. Geophys. Astrophys. Fluid Dyn. 51, 103–133.

Stone, P.H., 1972. A simplified radiative-dynamical model for the static stability of rotating atmospheres. J. Atmos. Sci. 29, 405–418.

Tandon, A., Garrett, C., 1996. On a recent parameterization of mesoscale eddies. J. Phys. Oceanogr. 26 (3), 406–416.

Theiss, J., 2004. Equatorward energy cascade, critical latitude, and the predominance of cyclonic vortices in geostrophic turbulence. J. Phys. Oceanogr. 34, 1663–1678.

Theiss, J., 2006. A generalized Rhines effect and storms on Jupiter. Geophys. Res. Lett. 33 (L08809). doi:10.1029/2005GL025379.

Treguier, A.M., Held, I.M., Larichev, V.D., 1997. Parameterization of quasigeostrophic eddies in primitive equation ocean models. J. Phys. Oceanogr. 27, 567–580.

Visbeck, M., Marshall, J., Haine, T., Spall, M., 1997. Specification of eddy transfer coefficients in coarse-resolution ocean circulation models. J. Phys. Oceanogr. 27, 381–402.

Zhai, X., Greatbatch, R.J., 2006a. Inferring the eddy-induced diffusivity for heat in the surface mixed layer using satellite data. Geophys. Res. Lett. 33 (L24607). doi:10.1029/2006GL027875.

Zhai, X., Greatbatch, R.J., 2006b. Surface eddy diffusivity for heat in a model of the northwest Atlantic Ocean. Geophys. Res. Lett. 33 (L24611). doi:10.1029/2006GL028712.